OPTICS

Resolving enantiomers using the optical angular momentum of twisted light

10.1126/sciadv.1501349

Ward Brullot, Maarten K. Vanbel, Tom Swusten, Thierry Verbiest*

Circular dichroism and optical rotation are crucial for the characterization of chiral molecules and are of importance to the study of pharmaceutical drugs, proteins, DNA, and many others. These techniques are based on the different interactions of enantiomers with circularly polarized components of plane wave light that carries spin angular momentum (SAM). For light carrying orbital angular momentum (OAM), for example, twisted or helical light, the consensus is that it cannot engage with the chirality of a molecular system as previous studies failed to demonstrate an interaction between optical OAM and chiral molecules. Using unique nanoparticle aggregates, we prove that optical OAM can engage with materials' chirality and discriminate between enantiomers. Further, theoretical results show that compared to circular dichroism, mainly based on magnetic dipole contributions, the OAM analog helical dichroism (HD) is critically dependent on fundamentally different chiral electric quadrupole contributions. Our work opens new venues to study chirality and can find application in sensing and chiral spectroscopy.

INTRODUCTION

For paraxial light beams, the total optical angular momentum (**J**) can be resolved in optical spin (**S**) and orbital (**L**) angular momentum (**J** = **S** + **L**). For left- and right-handed circularly polarized light, the optical spin angular momentum (SAM) assumes two defined values (**S** = −ħ or +ħ). The different interaction of optical SAM with right- (D) or left-handed (L) chiral molecules is the basis for optically resolving molecular enantiomers by the well-known circular dichroism (CD) or optical rotation techniques. The most common technique to study materials such as amino acids, proteins, DNA, RNA, and pharmaceutical drugs (*1*), but also nanoclusters (*2*), liquid crystals (*3*, *4*), and conjugated molecules (*5*, *6*), is CD. The main origin of CD is the interaction between electric and magnetic dipole contributions, leading to intrinsic chiral transitions, (*7*) although in oriented samples, interferences between electric dipole and quadrupole contributions can also contribute to conventional CD (*8*).

Optical orbital angular momentum (OAM) is a property of light beams with helical wavefronts, such as spatially twisted Laguerre-Gaussian (LG) beams, independent of light polarization (implying circularly polarized LG beams carry both optical OAM and SAM). Although SAM can assume only two defined values, OAM can have discrete values that are, in principle, unlimited (**L** = $l_z\hbar$), with the sign of l_z related to the handedness of the helical wavefront. Although intuitively expected, because the helical wavefronts are chiral, previous experimental studies on chiral molecules and liquid crystals demonstrated that optical OAM cannot engage with chiral matter (*9*, *10*). Theoretical work confirmed that OAM and chiral matter cannot interact through the commonly known electric or magnetic dipole transitions but does not exclude the possibility of interaction through higher-order interactions such as electric quadrupole fields (EQFs) (*11*–*15*). So until now, the optical OAM analog of CD, helical dichroism, has not been observed or described.

Recently, we observed strong EQFs in approximately 20-nm-thick plasmonic nanoparticle aggregates. These aggregates, synthesized in a layer-by-layer fashion and composed of silver, gold, and iron oxide nanoparticles of about 8 nm, show strong local EQFs due to near-field plasmon coupling between adjacent plasmonic nanoparticles (Fig. 1) (*16*, *17*). Layer-by-layer synthesis, using different plasmonic nanoparticles results in a structure with polar symmetry, that is, the near-field plasmon interactions and thus symmetry breaking occur predominantly in the direction perpendicular to the sample surface. The generated quadrupolar fields lead to nonreciprocal asymmetric transmission, that is, the dependence of optical transmission on the direction of light propagation (fig. S1) (*17*). Quadrupolarization-induced asymmetric transmission (Q-AT) is defined as the difference between measured intensities in forward and backward propagation direction divided by the average intensity (*17*)

$$\mathrm{AT} = I_{\mathrm{forward}} - I_{\mathrm{backward}} \Big/ \left[\frac{I_{\mathrm{forward}} + I_{\mathrm{backward}}}{2}\right]$$

The magnitude of the asymmetry is directly related to the efficiency of EQF generation (*17*). As such, measuring asymmetric transmission yields information on the strength of the EQFs generated in the material.

Here, we report the resolution of molecular enantiomers using the optical OAM of LG beams—helical dichroism. First, we prove that optical OAM indeed can interact with EQFs using LG light to probe unique plasmonic nanoparticle aggregates known to generate strong EQFs (*16*, *17*). In a second step, by adsorbing chiral molecules in the nanoparticle aggregates, we show that OAM can not only engage with molecular chirality through EQFs but also discriminate enantiomers far from the molecules' CD resonances (Fig. 1). This is demonstrated by measuring HD, that is, a difference in absorbance or transmission of left- and right-handed LG light for D and L enantiomers. Results from a developed phenomenological model establish that although CD requires chiral magnetic dipole contributions, considered the hallmark of chirality, differences in HD are only sensitive to the fundamentally different chiral electric quadrupole contributions.

RESULTS

LG beams with a chosen azimuthal index, and thus a discrete value of OAM (**L** = $l_z\hbar$), can be produced from linearly polarized 800-nm

Division Molecular Imaging and Photonics, Department of Chemistry, KU Leuven (University of Leuven), Celestijnenlaan 200D, Box 2425, 3001 Leuven, Belgium.
*Corresponding author. E-mail: thierry.verbiest@fys.kuleuven.be

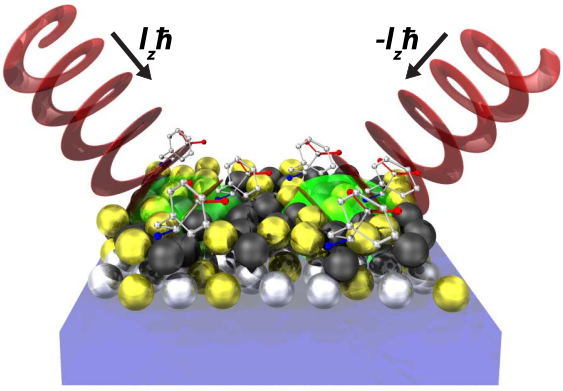

Fig. 1. Optical OAM exhibited by twisted LG light can discriminate molecular enantiomers through the strong EQFs generated in unique nanoparticle aggregates. In this not-to-scale schematic, the right- and left-handed LG beams (in red) interact differently (green shade) with the chiral molecules (stick-and-ball model) adsorbed to the nanoparticle aggregates.

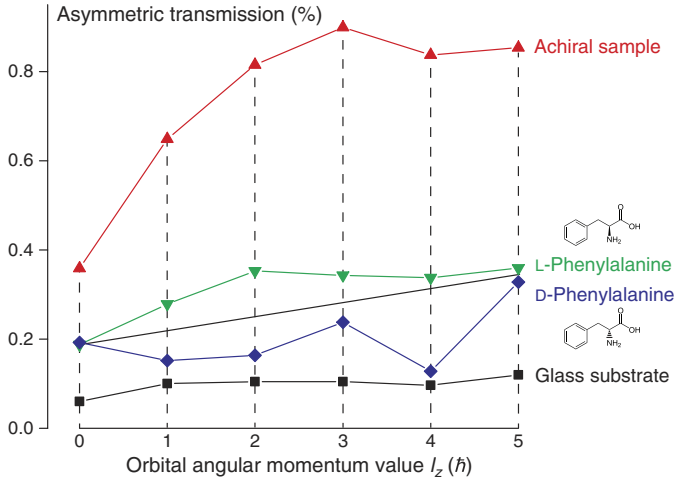

Fig. 2. Asymmetric transmission as a function of OAM value of the light beam. OAM can couple to EQFs, as evidenced by the shape of the achiral sample's curve (red upward triangles) compared to a glass substrate (black squares). OAM is also able to discriminate molecular enantiomers adsorbed in the plasmonic nanoparticle aggregates (green downward triangles, blue diamonds) based on different Q-AT values. Experimental errors are contained within the data points.

femtosecond pulsed laser light with a spatial light modulator (SLM) (Materials and Methods). Because we use linearly polarized light and measure total intensity, no conventional CD can be observed. By combining a stable laser source and averaging over 10 to 20 data points in 10 minutes of measurement time, the error on measurements could be kept well below 0.1%.

A clear proof of the interaction between OAM and EQFs was obtained by measuring the asymmetric transmission of an achiral aggregate sample as a function of l_z. Compared to a glass substrate, used as a reference because of negligible EQFs (Fig. 2, black squares) and regular Gaussian beams with $l_z = 0$, a significant increase in Q-AT is observed until $l_z = 3$, after which saturation is observed (Fig. 2, red upward triangles). Although the fundamental origin of the curve's shape remains to be elucidated, we postulate that the efficiency of electric quadrupolar field generation increases with increasing l_z. Because there is a limit on this efficiency, a saturation behavior is expected for larger l_z values (Q-AT ~ EQF/EQF_{MAX} ~ l_z).

To investigate the influence of molecular chirality on the Q-AT as a function of l_z, we adsorbed enantiopure D- and L-phenylalanine amino acid molecules in the aggregates. The amine functionality of these chiral enantiomers is capable of conjugating/attaching to the plasmonic nanoparticles, which allows them to adsorb in the aggregates. Adsorption of the molecules in the aggregates was confirmed using UV (ultraviolet)–visible spectroscopy, as the near-field coupling feature slightly red-shifted and broadened (fig. S2). Further, the measured asymmetric transmission significantly decreased due to a decrease in near-field coupling intensity. No CD signal was measured in the 300- to 850-nm spectral range, because the molecular phenylalanine CD features are in the UV and the number of chiral molecules in the very thin films is too small to generate a measurable CD response (fig. S3).

Remarkably, OAM-carrying light beams mediated by EQFs are not only sensitive to chirality but also capable of resolving molecular enantiomers. This is illustrated by measurements of Q-AT as a function of l_z for the chiral (D and L) samples (Fig. 2, green downward triangles, blue diamonds). A clearly different response from both enantiomers is observed when optical OAM is present ($l_z \neq 0$), which can be used to resolve enantiomers. For regular Gaussian beams with $l_z = 0$, the measured Q-AT is equal for both the D- and L-phenylalanine samples. This proves that OAM is required for enantiomeric resolution.

The equal signal levels were expected because no CD signal was measured and we used linearly polarized light. Further, this equality shows that intersample variations must be limited.

Because the Q-AT, as a function of the l_z curves, corresponds closely to mirror images over the average, it is possible to attribute a sign and relative magnitude to the molecular enantiomers and assign them. Small sample-to-sample variations in the plasmonic nanoparticle aggregate synthesis, as described in previous publications, explain the deviations from perfect mirror symmetry of the enantiomers (*16*, *17*).

To explain the origin of the observed difference in Q-AT for enantiomers ($AT_D - AT_L$), we developed a phenomenological model, which takes into account electric dipole, magnetic dipole, and electric quadrupole contributions to the optical response of the sample. A full description of the model and the results of the analysis can be found in the Supplementary Materials. We find that enantiomers react differently due to interactions between polar electric quadrupole (χ^{eq}_{polar}), which change sign when the propagation direction changes, and chiral magnetic dipole (χ^{em}_{chiral}) or chiral electric quadrupole (χ^{eq}_{chiral}) contributions, which change sign when the enantiomers are switched (see the Supplementary Materials for analysis)

$$AT_D - AT_L \sim \chi^{eq}_{polar}\chi^{em}_{chiral} + \chi^{eq}_{polar}\chi^{eq}_{chiral}$$

As follows from the analysis, the difference ($AT_D - AT_L$) becomes 0, as experimentally observed (Fig. 2), for linearly polarized plane wave Gaussian beams with $l_z = 0$.

The critical dependence of the difference between enantiomers on the crucial electric quadrupole contributions is in contrast to conventional CD measurements where the difference is commonly due to χ^{em}_{chiral} contributions. The convolution or "interference" of polar and chiral contributions for LG light also explains why resolution of enantiomers is possible far from the molecular CD resonances in the UV region.

Knowing that EQFs are the mediator between OAM and molecular chirality, it is also possible to directly measure the difference in transmission for right-handed ($+l_z$) and left-handed ($-l_z$) helical light carrying OAM. This is analogous to CD for right- and left-handed circularly polarized light carrying SAM. Because of this analogy, we define "helical dichroism" as the difference in transmission or absorption of right-handed (+) and left-handed (−) helical light or

$$\mathrm{HD} = \frac{I_+ - I_-}{\left[\frac{I_+ - I_-}{2}\right]}$$

HD measurements as a function of l_z show a clear discrimination between molecular enantiomers adsorbed in the nanoparticle aggregates (Fig. 3). Switching the enantiomer switches the sign but retains, to large extent, the absolute value of the measured HD. Hence, the responses of both enantiomers are mirror images over the 0% HD line. The HD versus l_z curves show no resolving power at $l_z = 0$, have a maximum absolute value for $l_z = 1$, and have a crossover point between $l_z = 2$ and $l_z = 3$. Because regular differential absorption/transmission values for CD are in the 0.01 to 0.1% range, the measured HD values of up to 0.6% HD are significant (*18*).

Although the fundamental origin of this behavior needs to be further investigated, the results of the phenomenological model show (a full description of the model and the results of the analysis can be found in the Supplementary Materials) that the differences in HD for different enantiomers can be solely attributed to terms with chiral electric quadrupole contributions. For $l_z = 0$, the difference ($\mathrm{HD_D} - \mathrm{HD_L}$) becomes 0, as experimentally observed (Fig. 3), because measuring a difference between $+l_z$ and $-l_z$ requires $l_z \neq 0$

$$\mathrm{HD_D} - \mathrm{HD_L} \sim \chi^{ee}_{\mathrm{isotropic}}\chi^{eq}_{\mathrm{chiral}} + \chi^{eq}_{\mathrm{polar}}\chi^{eq}_{\mathrm{chiral}}$$

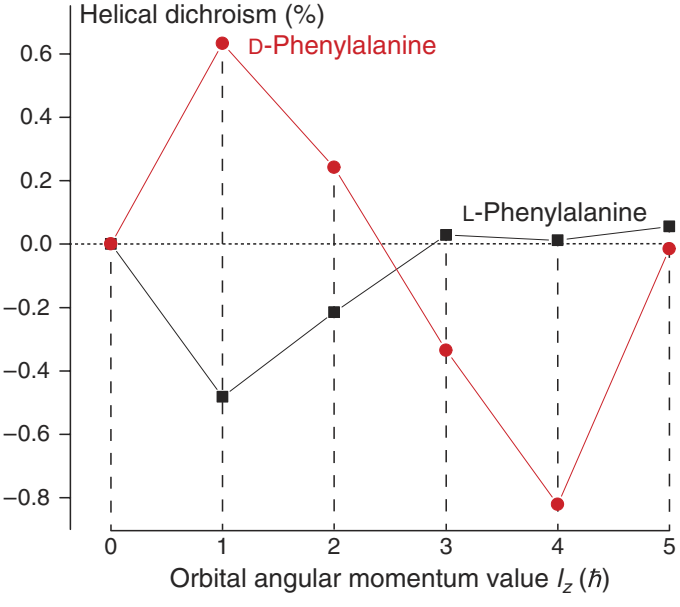

Fig. 3. HD measurements as a function of OAM value, that is, measuring the difference in transmission for right- and left-handed helical light shows clear discrimination of molecular enantiomers. Experimental errors are contained within the data points.

The first term in the difference equation, $\chi^{ee}_{\mathrm{isotropic}}\chi^{eq}_{\mathrm{chiral}}$, does not require a polar structure. This is because $\chi^{ee}_{\mathrm{isotropic}}$, the linear electric dipole susceptibility and related to the refractive index of the structure, is allowed for all sample symmetries. So hypothetically speaking, it is possible to resolve enantiomers of molecules exhibiting large $\chi^{eq}_{\mathrm{chiral}}$ based on differences in HD in isotropic samples, such as solutions or dispersions of chiral structures. Possible candidates might be helically shaped molecules such as DNA, proteins, or peptides.

Although the developed phenomenological model proves that chiral electric quadrupole contributions are a prerequisite for observing HD, it does not provide information on the shape of the HD curves as a function of OAM value. For this, a model that studies the fundamental origins of HD needs to be developed. However, as a function of OAM value, the differential HD ($\mathrm{HD_D} - \mathrm{HD_L}$) switches sign (see Fig. 3, crossover point). Because the phenomenological model shows that this difference depends on two terms, $\chi^{ee}_{\mathrm{isotropic}}\chi^{eq}_{\mathrm{chiral}}$ and $\chi^{eq}_{\mathrm{polar}}\chi^{eq}_{\mathrm{chiral}}$, it implies that these terms carry a different sign and that the balance between these terms shifts with increasing OAM value. Further, because the sign and magnitude of these terms are material-specific, it should be possible to use the shape of the HD curves for material identification purposes.

DISCUSSION

The unique dependence on only electric quadrupole contributions shows that magnetic dipole contributions, considered the hallmark for chiral behavior and the basis of CD spectroscopy, are not required to resolve molecular enantiomers. Further, combining CD and HD measurements enables us to untangle the chiral magnetic dipole and chiral electric quadrupole contributions to the total chiral signal. Untangling these contributions might prove useful in chiral systems with large electric field gradients, yielding large EQFs, such as chiral molecules in the vicinity of plasmonic nanoparticles (*19*, *20*).

By demonstrating that OAM can interact with EQFs and that OAM can resolve molecular enantiomers through this interaction, and by applying it to measure HD and showing that differences in HD are solely due to electric quadrupole contributions, our work opens new ways to study chiral molecules and materials. Interesting venues for further investigation are the wavelength dependence of the interactions, the influence of the nature of the chiral molecule, and the relationship between SAM and OAM in chiral samples with strong EQFs. Besides fundamental interests, enantiomeric resolution by OAM has the potential for application in, for example, sensing or HD spectroscopy.

MATERIALS AND METHODS

UV-visible and CD spectroscopy measurements

UV-visible measurements were done on a PerkinElmer Lambda 900, and CD measurements on a Jasco J-810 spectropolarimeter.

Optical setup for measurements using LG beams

A schematic representation is shown in Fig. 4. The light source was a 150-fs pulsed Spectra-Physics Mai Tai Ti:Sapphire laser at 800-nm wavelength with 1.09 W of output power. After the beam was chopped at a frequency of 770 Hz, passed through a pinhole, and reflected by two mirrors, the laser beam intensity was attenuated by a half-wave

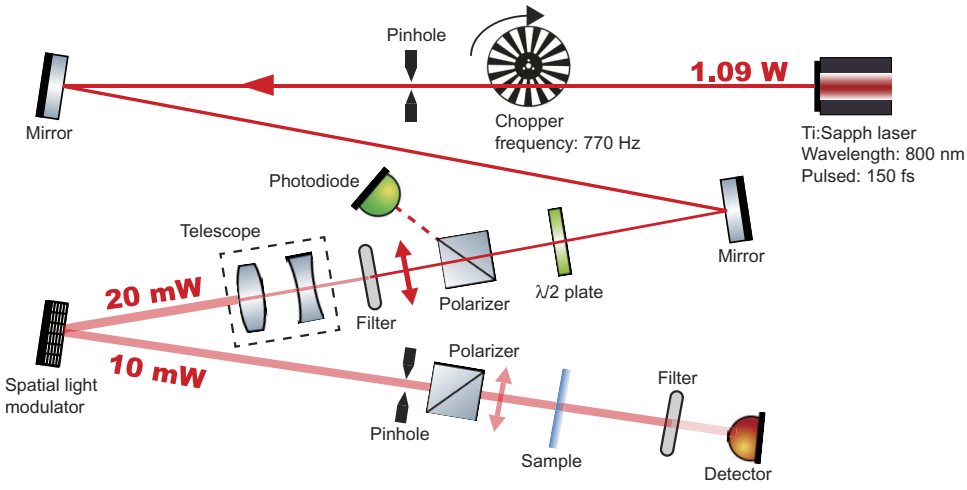

Fig. 4. Schematic representation of the optical setup used for measurements with LG beams.

plate/polarizer (p-polarization) combination followed by neutral density filters. A laser reflection from the polarizer was detected by a photodiode and used to measure the stability of the laser. After the neutral density filter, the beam was expanded by a telescope and reaches a calibrated SLM (HOLOEYE Pluto system) under a small angle with 20-mW power. Precalculated phase masks to generate LG beams with different OAM values were fed to the SLM by a computer. Light reflected from the SLM (10 mW) then passed a pinhole to remove higher-order diffraction modes and a second polarizer to ensure p-polarized light. The sample was mounted on a motorized rotation stage to ensure reproducible 180° rotation of the sample for asymmetric transmission measurements, passed another neutral density filter, and then focused with an anti-reflection coated lens on to the detecting photodiode. The power levels for the left- and right-handed LG beams after the SLM were checked to be equal within experimental error. This excludes contributions from different power levels, such as nonlinear optical, to the observed effect.

The photodiode signal was fed to a lock-in detector operating in external reference mode with input from the mechanical chopper (770 Hz). Data acquisition was done using a LabVIEW program. Used time constant was 1 s, and 10 to 20 data points were gathered over 10 min per measurement. The gathered data points were averaged per measurement and used as such. This approach excludes time-dependent effects to contribute to the measured signals.

Because of the homogeneity of the produced samples and the use of nonfocused LG beams, which allows probing a large region, the effect is not dependent on the measured spatial region of the samples.

The spatial intensity profiles of the produced LG beams detected by a webcam as a function of OAM value and handedness are shown in fig. S4. Note that the inhomogeneities in the beam outside of the central annulus are due to an imperfect detection system. Spatial intensity profiles of the LG beams were as expected.

Synthesis of achiral plasmonic nanoparticle aggregates

Achiral samples showing asymmetric transmission were prepared according to a previously reported protocol (*16*, *17*). Full experimental results can be found in these references.

By self-assembling small plasmonic silver and gold nanoparticles together with high–refractive index iron oxide nanoparticles on glass substrates, near-field coupled aggregates of nanoparticles are obtained. This self-assembly process provides optically isotropic and partially transparent samples that show nonreciprocal asymmetric transmission in a reproducible way.

Briefly summarized, glass substrates are first functionalized with aminopropyltrimethoxysilane (APTMS), providing amine functionality as an attachment anchor for the first layer of plasmonic silver nanoparticles. This first low-density silver nanoparticle (9.6 ± 0.2 nm, synthesis with sodium citrate and sodium borohydride) layer is attached through self-assembly by shaking a silver nanoparticle dispersion for 2 hours in the presence of the functionalized substrate. A second layer, consisting of high–refractive index iron oxide nanoparticles (7.9 ± 2.4 nm) prefunctionalized with APTMS, is added to the first layer by self-assembly. These iron oxide nanoparticles act as "glue" between the first-layer silver and third-layer gold nanoparticles and further as a local refractive index enhancer. This last property enhances the near-field interactions within the nanoparticle aggregates. Last, a high-density gold nanoparticle (9.2 ± 1.3 nm) layer is added, completing the samples. The end result is a substrate covered with asymmetric near-field coupled silver-gold nanoparticle aggregates in a high–refractive index environment. The aggregates' principal exes are on average perpendicular to the substrates' surface.

Because initially both sides of the substrates are covered with nanoparticle aggregates, one side is cleaned by mechanically removing the coating.

Preparation of chiral plasmonic nanoparticle aggregates

Enantiomerically pure chiral plasmonic nanoparticle aggregate samples were produced by submersing achiral samples in a 1 mM aqueous solution of D- or L-phenylalanine (molecules were acquired from Sigma-Aldrich and used as such) while shaking (300 rpm) for 2 hours, after which the samples were rinsed with water and stored in methanol.

SUPPLEMENTARY MATERIALS

Supplementary material for this article is available at http://advances.sciencemag.org/cgi/content/full/2/3/e1501349/DC1

Fig. S1. Transmission and asymmetry of transmission spectra for the achiral samples.

Fig. S2. Transmission and asymmetry of transmission spectra for the chiral samples.

Fig. S3. CD spectra of the achiral and chiral samples in both forward and backward direction.
Fig. S4. Spatial intensity profiles of the produced LG beams.
Fig. S5. Configuration of the system with visualization of the coordinate axes.
Model. Phenomenological model for discrimination of molecular enantiomers by LG light.
References (*21*–*24*)

REFERENCES AND NOTES

1. R. Garret, C. Grisham, *Biochemistry* (Cengage Learning, Belmont, CA, ed. 5, 2012).
2. S. Knoppe, T. Bürgi, Chirality in thiolate-protected gold clusters. *Acc. Chem. Res.* **47**, 1318–1326 (2014).
3. I. Dierking, Chiral liquid crystals: Structures, phases, effects. *Symmetry* **6**, 444–472 (2014).
4. K. Binnemans, Ionic liquid crystals. *Chem. Rev.* **105**, 4148–4204 (2005).
5. D. Cornelis, E. Franz, I. Asselberghs, K. Clays, T. Verbiest, G. Koeckelberghs, Interchromophoric interactions in chiral X-type π-conjugated oligomers: A linear and nonlinear optical study. *J. Am. Chem. Soc.* **133**, 1317–1327 (2011).
6. F. Monnaie, W. Ceunen, J. De Winter, P. Gerbaux, V. Cocchi, E. Salatelli, G. Koeckelberghs, Synthesis and transfer of chirality in supramolecular hydrogen bonded conjugated diblock copolymers. *Macromolecules* **48**, 90–98 (2015).
7. T. Verbiest, K. Clays, V. Rodriguez, *Second-Order Nonlinear Optical Characterization Techniques: An Introduction* (CRC Press, Boca Raton, FL, 2009).
8. D. P. Craig, T. Thirunamchandran, *Molecular Quantum Electrodynamics: An Introduction to Radiation-Molecule Interactions* (Dover Publications, Mineola, NY, 1998).
9. F. Araoka, T. Verbiest, K. Clays, A. Persoons, Interactions of twisted light with chiral molecules: An experimental investigation. *Phys. Rev. A* **71**, 055401 (2005).
10. W. Löffler, D. J. Broer, J. P. Woerdman, Circular dichroism of cholesteric polymers and the orbital angular momentum of light. *Phys. Rev. A* **83**, 065801 (2011).
11. M. Babiker, C. Bennett, D. L. Andrews, L. C. Dávila Romero, Orbital angular momentum exchange in the interaction of twisted light with molecules. *Phys. Rev. Lett.* **89**, 143601 (2002).
12. D. L. Andrews, L. C. Dávila Romero, M. Babiker, On optical vortex interactions with chiral matter. *Opt. Commun.* **237**, 133–139 (2004).
13. M. M. Coles, D. L. Andrews, Chirality and angular momentum in optical radiation. *Phys. Rev. A.* **85**, 063810 (2012).
14. P. K. Mondal, B. Deb, S. Majumder, Angular momentum transfer in interaction of Laguerre-Gaussian beams with atoms and molecules. *Phys. Rev. A.* **89**, 063418 (2014).
15. E. Karimi, S. A. Schulz, I. De Leon, H. Qassim, J. Upham, R. W. Boyd, Generating optical orbital angular momentum at visible wavelengths using a plasmonic metasurface. *Light Sci. Appl.* **3**, e167 (2014).
16. W. Brullot, R. Strobbe, M. Bynens, M. Bloemen, P.-J. Demeyer, W. Vanderlinden, S. De Feyter, V. K. Valev, T. Verbiest, Layer-by-layer synthesis and tunable optical properties of hybrid magnetic–plasmonic nanocomposites using short bifunctional molecular linkers. *Mater. Lett.* **118**, 99–102 (2014).
17. W. Brullot, T. Swusten, T. Verbiest, Broadband nonreciprocal quadrupolarization-induced asymmetric transmission (Q-AT) in plasmonic nanoparticle aggregates. *Adv. Mater.* **27**, 2485–2488 (2015).
18. A. J. Adler, N. J. Greenfield, G. D. Fasman, Circular dichroism and optical rotatory dispersion of proteins and polypeptides. *Methods Enzymol.* **27**, 675–735 (1973).
19. A. O. Govorov, Z. Fan, P. Hernandez, J. M. Slocik, R. R. Naik, Theory of circular dichroism of nanomaterials comprising chiral molecules and nanocrystals: Plasmon enhancement, dipole interactions, and dielectric effects. *Nano Lett.* **10**, 1374–1382 (2010).
20. R.-Y. Wang, P. Wang, Y. Liu, W. Zhao, D. Zhai, X. Hong, Y. Ji, X. Wu, F. Wang, D. Zhang, W. Zhang, R. Liu, X. Zhang, Experimental observation of giant chiroptical amplification of small chiral molecules by gold nanosphere clusters. *J. Phys. Chem. C.* **118**, 9690–9695 (2014).
21. J. D. Jackson, *Classical Electrodynamics* (John Wiley & Sons, New York, 1962).
22. A. Cerjan, C. Cerjan, Orbital angular momentum of Laguerre–Gaussian beams beyond the paraxial approximation. *J. Opt. Soc. Am. A.* **28**, 2253–2260 (2011).
23. R. J. Potton, Reciprocity in optics. *Reports Prog. Phys.* **67**, 717–754 (2004).
24. U. Schlagheck, The significance of quadrupole-electric coefficients for the optical properties of nonmagnetic crystals. *Zeitschrift für Phys.* **266**, 313–317 (1974).

Acknowledgments: We would like to thank S. Vandendriessche for calculating and preparing the LG phase masks for the SLM and C. Verstraete for practical assistance during measurements. **Funding:** This work was supported by FWO-Vlaanderen through grant G.0C02.13 and by KU Leuven (University of Leuven) through grant IDO/11/007 and postdoctoral fellowships for W.B. and M.K.V. T.V. is also a member of the Institute for Nanoscale Physics and Chemistry (KU Leuven). **Author contributions:** T.V., W.B., and M.K.V. conceived the experiment. T.S. synthesized and modified the nanoparticle aggregates, adsorbed chiral molecules into the structures, and measured UV-visible spectral data. W.B. and M.K.V. performed the LG beam experiments and analyzed the results. W.B. measured the CD spectra. T.V. supervised the experiments. All authors discussed the data and contributed to writing the paper. **Competing interests:** The authors declare that they have no competing interests. **Data and materials availability:** All data needed to evaluate the conclusions in the paper are present in the paper and/or the Supplementary Materials. Additional data related to this paper may be requested from the authors.

Submitted 30 September 2015
Accepted 17 January 2016
Published 11 March 2016
10.1126/sciadv.1501349

Citation: W. Brullot, M. K. Vanbel, T. Swusten, T. Verbiest, Resolving enantiomers using the optical angular momentum of twisted light. *Sci. Adv.* **2**, e1501349 (2016).

Resolving enantiomers using the optical angular momentum of twisted light

Ward Brullot, Maarten K. Vanbel, Tom Swusten and Thierry Verbiest

Sci Adv **2** (3), e1501349.
DOI: 10.1126/sciadv.1501349